Nucleic Acids Research

Characterization of DNA structures by Raman spectroscopy: high-salt and low-salt forms of double helical poly(dG-dC) in H₂O and D₂O solutions and application to B, Z and A-DNA*

J.M.Benevides and G.J.Thomas,Jr. +

Department of Chemistry, Southeastern Massachusetts University, North Dartmouth, MA 02747, USA

ABSTRACT

Raman spectra of poly(dG-dC)·poly(dG-dC) in D_2O solutions of high (4.0M NaCl) and low-salt (0.1M NaCl) exhibit differences due to different nucleotide conformations and secondary structures of Z and B-DNA. Characteristic carbonyl modes in the 1600-1700 cm^{-1} region also reflect differences in base pair hydrogen bonding of the respective GC complexes. Comparison with A-DNA confirms the uniqueness of C=O stretching frequencies in each of the three DNA secondary structures. Most useful for qualitative identification of B, Z and A-DNA structures are the intense Raman lines of the phosphodiester backbone in the 750-850 cm^{-1} region. A conformation-sensitive guanine mode, which yields Raman lines near 682, 668, or 625 cm^{-1} in B (C2'-endo, anti), A (C3'-endo, anti) or Z (C3'-endo, syn) structures, respectively, is the most useful for quantitative analysis. In D_2O, the guanine line of Z-DNA is shifted to 615 cm^{-1}, permitting its detection even in the presence of proteins.

INTRODUCTION

An unusual conformation for the synthetic DNA containing alternating guanine and cytosine bases, poly(dG-dC)·poly(dG-dC), was first demonstrated by Pohl and co-workers using techniques of circular dichroism (1) and laser Raman spectroscopy (2). Both the CD and Raman spectra of the polymer suggested a conformation in solutions of high salt (4M NaCl) which differed from the conventional B-DNA or right-handed helical structure normally occurring in solutions of lower salt concentration. Recent X-ray diffraction analyses of single crystals of the hexanucleotide duplex, d(CGCGCG)·d(CGCGCG), have revealed a left-handed helical structure containing syn conformers of guanine and a zig-zag backbone designated Z-DNA (3,4). Comparison of the Raman spectrum of the authenticated Z-DNA oligomer with the Raman spectrum of the high-salt form of poly(dG-dC)· poly(dG-dC) has confirmed a Z-DNA structure for the latter in aqueous solution (5). Raman spectroscopy has also been employed to detect Z-DNA domains in restriction fragments containing alternating G and C residues

in extended sequence (6). These studies indicate the utility of the Raman
effect for identifying Z conformers in oligomeric and polymeric
structures, and for distinguishing Z–DNA and B–DNA structures from one
another.

The usefulness of Raman spectroscopy for the identification of
different DNA structures is greatly enhanced by the availability of
spectra of both deuterated (D_2O) and non-deuterated (H_2O) solution forms
(7,8). At present there is no detailed study of the Raman spectrum of
poly(dG–dC)·poly(dG–dC) in D_2O solution, although there exist several such
studies of the canonical A–DNA and B–DNA structures (7–10). In this paper
we report and discuss the Raman spectra of deuterated forms of the Z–DNA
model, poly(dG–dC)·poly(dG–dC). The data are compared with those of the
deuterated B structure of this polynucleotide, also not previously
reported, and with more recent results obtained on guanine and cytosine
model compounds (11,12).

Methods of Raman difference spectroscopy have been employed to
collect data of higher precision than could be obtained without the use of
computer subtraction techniques. Difference spectroscopy is here applied
to both deuterated and nondeuterated samples to reveal previously obscured
or hidden frequencies characteristic of the Z–DNA structure. We have also
exploited the fact that D_2O, unlike H_2O, gives virtually no solvent
interference in either the structurally informative double-bond stretching
region (1500–1800 cm^{-1}) or in the region of aliphatic CH stretching
frequencies (2800–3000 cm^{-1}). A number of new conformation-sensitive
Raman lines have been detected in these intervals.

EXPERIMENTAL METHODS

Poly(dG–dC)·poly(dG–dC) was purchased as the sodium salt from PL
Biochemicals and required no further purification to yield Raman spectra
free of interfering impurities or background fluorescence. The
polynucleotide was dissolved to 40 mg/ml in either H_2O or D_2O (99.8%,
Aldrich Chemical) which contained also the appropriate concentration of
NaCl to yield either the B–DNA (0.1M NaCl) or Z–DNA (4.0M NaCl) structure.
All solutions were adjusted to pH or pD 7.0 prior to loading into sample
cells (Kimax #34507 capillaries). Further details of sample handling
procedures have been described previously (7).

All Raman spectra were excited with 200 milliwatts of 514.5 nm
radiation from an argon laser (Coherent Radiation, Model CR-2), and were

recorded on a Spex Ramalog spectrophotometer employing digital photon counting under the control of a North Star Horizon II microcomputer. A similarly computerized spectrophotometer has been described by Li et al. (13). Ordinarily, the spectral data were collected at 1.0 cm^{-1} intervals and with an integration time of 1.5 seconds. The spectral slit width was 8.0 cm^{-1} and the sample temperature was 32°C, unless indicated otherwise. Raman frequencies are accurate to ± 2 cm^{-1}.

The Raman spectra illustrated below are the computer average of five or more scans recorded consecutively and displayed individually on a video terminal. Hard copies were produced on a Houston Complot printer interfaced to the microcomputer.

For the computer subtraction of solvent background from spectra of polynucleotide solutions, the Raman spectra of H_2O and D_2O solutions of NaCl (0.1M and 4.0M) were recorded at the same instrument conditions. Following the subtraction of solvent, some of the spectra were smoothed by a least squares fit of third order polynomials to overlapping fifteen point regions (14). This procedure, which reduced the spectral noise
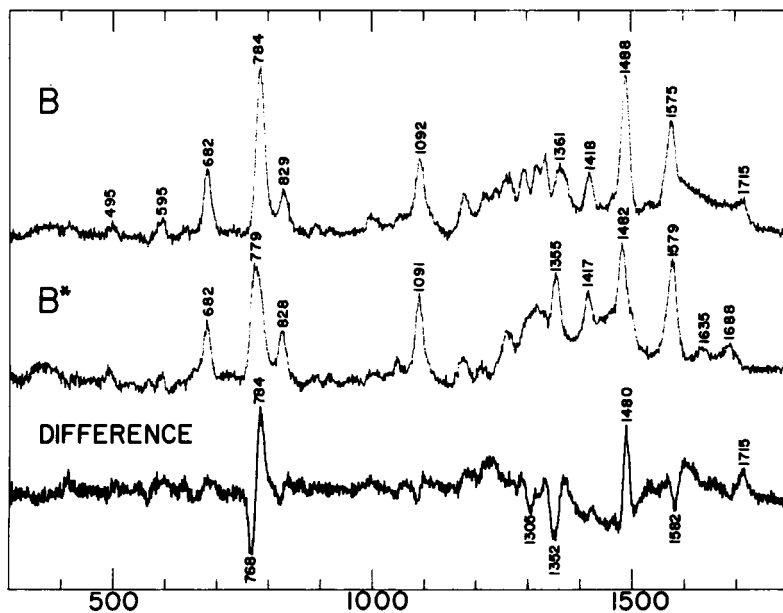

FIGURE 1: Raman spectra in the region 300-1800 cm^{-1} of H_2O (B) and D_2O (B*) solution forms of poly(dG–dC)·poly(dG–dC) and the corresponding difference spectrum (B – B*), each in 0.1M NaCl solution at 40 mg/ml, pH7 and 32°C. Other conditions are described in the text.

considerably, did not alter measurably the Raman line frequencies or
intensities. To aid in analyzing the spectral effects of deuteration and
of the B-to-Z structure transition, the following difference spectra were
computer generated: B-DNA minus B*-DNA, Z-DNA minus Z*-DNA, B-DNA minus Z-
DNA and B*-DNA minus Z*-DNA. (Here, asterisks are used to designate
deuterated polynucleotides, i.e. polynucleotides in D_2O solutions.)

RESULTS AND DISCUSSION

Fig. 1 shows the Raman spectra in the region 300 to 1800 cm^{-1} of B
and B* structures and the difference spectrum B - B*. Corresponding data
for Z structures are shown in Fig. 2. The Raman spectra of aqueous
poly(dG-dC)·poly(dG-dC) in low (B) and high (Z) salt forms, and their
difference spectrum (B - Z), are shown in Fig. 3. The spectra of D_2O
solutions of the low (B*) and high (Z*) salt forms, and their
corresponding difference spectrum (B*- Z*), are shown in Fig. 4. Also
shown in Fig. 4 is the CH stretching region (2800-3200 cm^{-1} interval),
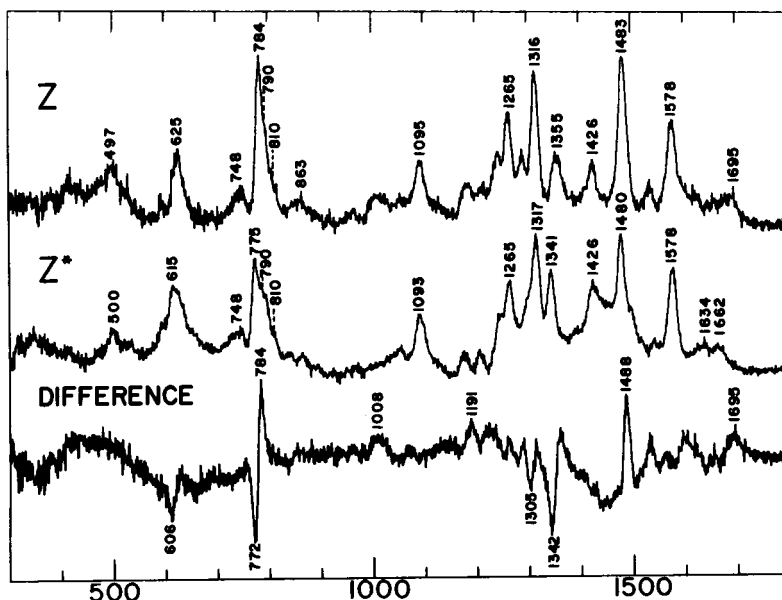which is not obscured by the D_2O solvent. Figs. 1 and 2 reveal the

FIGURE 2: Raman spectra in the region 300-1800 cm^{-1} of H_2O (Z) and D_2O
(Z*) solution forms of poly(dG-dC)·poly(dG-dC) and the corresponding
difference spectrum (Z - Z*), each in 4.0M NaCl solution at 40 mg/ml, pH7
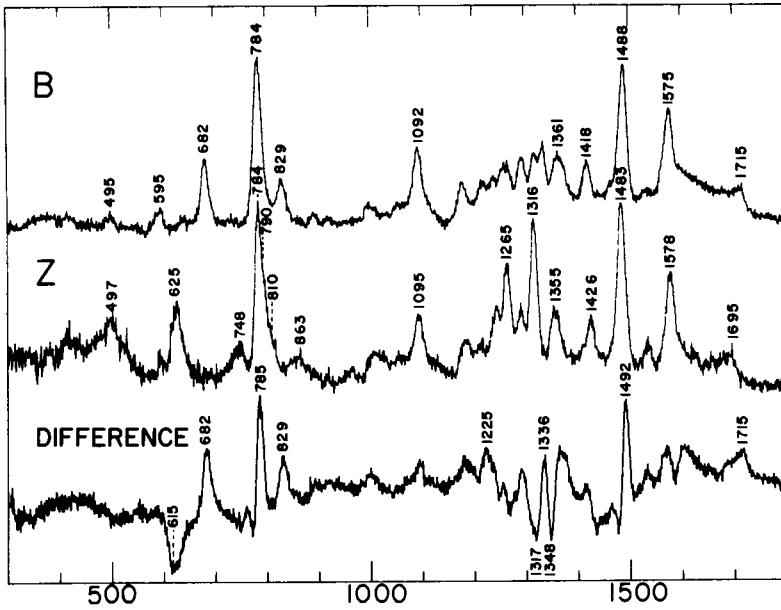and 32°C. Other conditions are described in the text.

FIGURE 3: Raman spectra in the region 300-1800 cm^{-1} of B and Z forms of poly(dG-dC)·poly(dG-dC) and their difference spectrum.

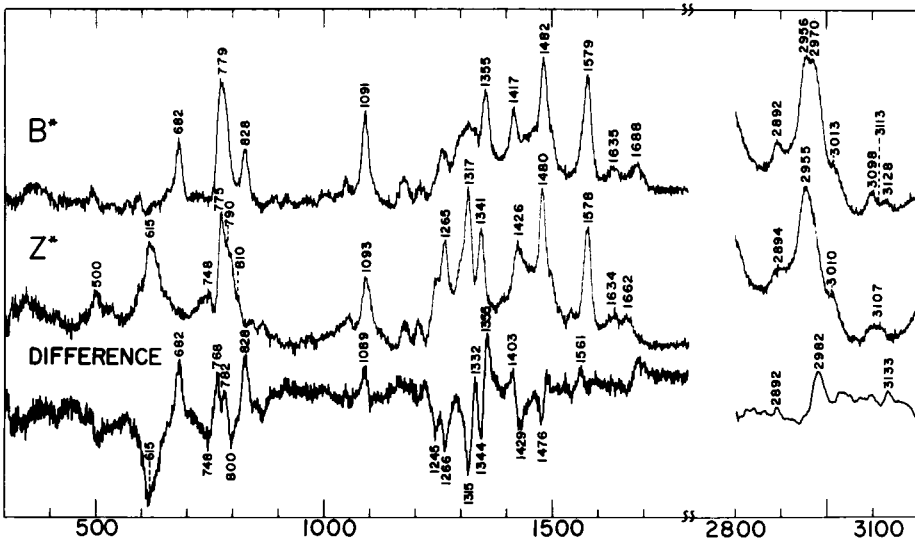FIGURE 4: Raman spectra in the region 300-1800 cm^{-1} of B* and Z* forms of poly(dG-dC)·poly(dG-dC) and their difference spectrum. Also included is the region of aliphatic and aromatic CH stretching vibrations (2800-3200 cm^{-1}).
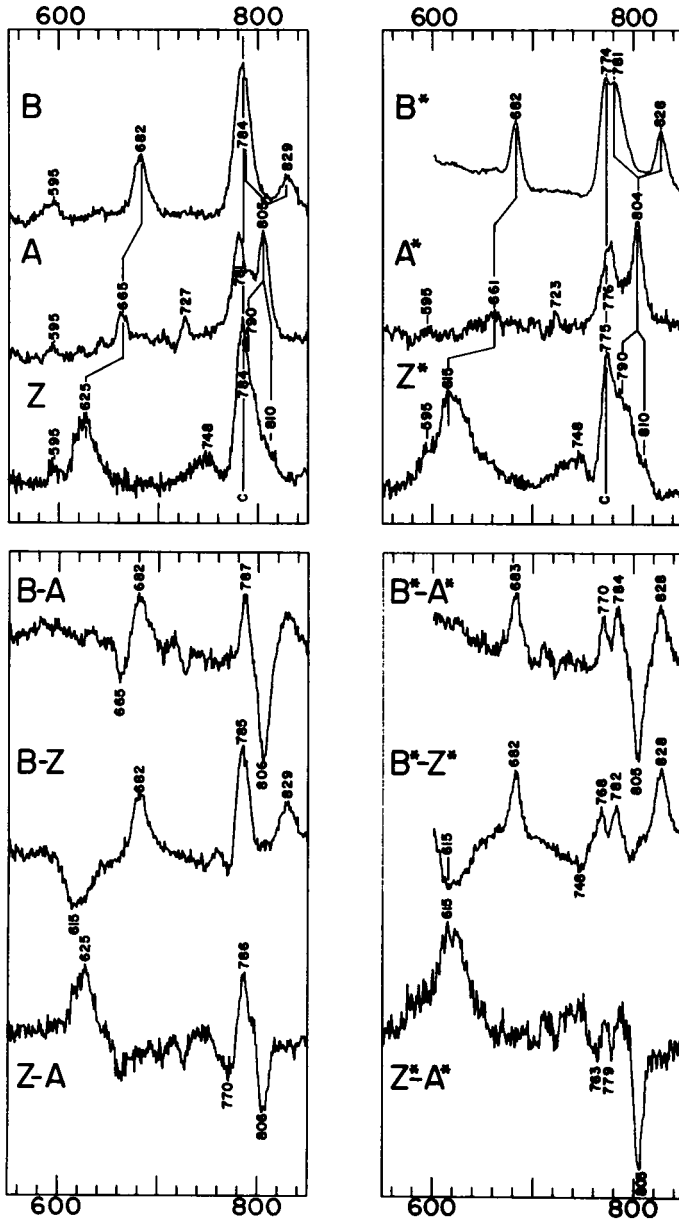
FIGURE 5: Raman spectra in the region 550–850 cm^{-1} of B, A and Z structures (left), and of B*, A* and Z* structures (right) of DNA, and their corresponding difference spectra. Data from A and A* fiber structures are from reference 8. (Note that A-DNA also contains a prominent adenine line at 727 cm^{-1}, not present in the B and Z structures.)

effects of deuteration on both secondary structures while Figs. 3 and 4
show the effects of the structure transition upon all Raman line
frequencies and intensities of the copolynucleotide. Fig. 5 contains the
region 550-850 cm^{-1} of Z, B and A structures, recorded at high spectral
resolution to show the important backbone and base vibrational modes which
permit straightforward discrimination of all three DNA structures from one
another.

In order to generate difference data in a manner consistent with that
employed previously for A and B-DNA (8), all Raman spectra, prior to
subtraction, were normalized to yield the same integrated intensity of the
purine band centered at approximately 1575 cm^{-1}, as measured from the
straight line connecting its wings near 1550 and 1600 cm^{-1}. The rationale
for this choice of Raman intensity normalization has been given previously
(8), and rests upon the demonstrated invariance of the integrated
intensity of the 1575 cm^{-1} line to structure and deuteration changes of
DNA, RNA and synthetic polynucleotides.

Effects of Deuteration.

Fig. 1 shows that the guanine ring mode at 682 cm^{-1}, which is known
to be sensitive to the sugar ring pucker (11), is only slightly affected
by deuteration of the B structure. Other prominent Raman frequencies
which are not greatly affected by deuteration are the phosphate dioxy
stretch at 1092 cm^{-1} and the phosphodiester antisymmetric stretch at 829
cm^{-1}. These results confirm those observed for native B-DNA (8).
Virtually all other intense Raman lines of the B structure undergo either
frequency shift or intensity change, or both, with deuteration. The
greatest intensity change occurs in the band centered at 784 cm^{-1} in the B
structure, which is shifted to lower frequency upon deuteration, as is
evident in the difference spectrum of Fig. 1. We interpret this result as
follows.

The 784 cm^{-1} band of B-DNA is actually the composite of two major
bands, one due to the cytosine ring (breathing mode, ca. 780 cm^{-1}
(12,15)), the other due to the B-DNA backbone (phosphodiester symmetric
stretch, ca. 785 cm^{-1} (8-10)). The former is deuteration sensitive
(7,12); the latter is less so (8). Consequently, the difference spectrum
shows positive and negative peaks at the approximate positions of the
cytosine ring modes in B and B* structures, respectively. We may conclude
that the 785 cm^{-1} phosphodiester frequency, like the 829 and 1092 cm^{-1}
phosphate group modes, is virtually fully compensated in the difference

spectrum of Fig. 1. A high resolution scan of this region of the B[*]
spectrum clearly resolves the two components of the composite 784 cm^{-1}
band in the D_2O solution spectrum (Fig. 5).

The intense Raman line at 1488 cm^{-1}, assigned to guanine (15), shifts
to 1482 cm^{-1} upon deuteration of exocyclic NH and NH_2 groups of the
guanine ring. This highly characteristic purine ring mode involves also
the 8C–H bending coordinate and has been shown to shift still further to
lower frequency (ca. 1465 cm^{-1}) with 8C deuteration (16). Accordingly,
the absence of a strong negative band near 1465 cm^{-1} in the difference
spectrum of Fig. 1 indicates that no appreciable deuteration of the 8C
group occurs within the time frame of accumulation of these Raman spectral
data.

In the region 1500–1800 cm^{-1}, the so-called double-bond region, the
carbonyl group stretching frequencies of G and C are expected to occur
with significant Raman intensity. However, interpretation of the data
from H_2O solutions in this region is complicated by two factors: coupling
of C=O stretching with NH and NH_2 bending modes in G and C, and
interference from the Raman band of liquid H_2O near 1645 cm^{-1}. The latter
is largely ameliorated by computer subtraction of the solvent spectrum;
however, vibrational coupling and overlap of NH bending modes are not
easily compensated. Consequently, we look to the D_2O solution spectrum of
Fig. 1 for the characteristic C=O stretching frequencies of the low-salt
structure (B[*]).

The line at 1688 cm^{-1} is assigned to the guanine 6C=O stretch and the
line at 1635 cm^{-1} to the cytosine 2C=O stretch, by analogy with
mononucleotide spectra (15). Yet, both of these frequencies are
significantly shifted from their respective values in corresponding
mononucleotides and single-stranded polynucleotides (e.g., 1650 cm^{-1} in
CMP and poly(rC), and 1675 cm^{-1} in GMP and poly(rG) (8,12,15,17)). As
shown by Howard et al. (18), the C=O frequencies of hydrogen-bonded GC
pairs in polynucleotides can be explained in terms of interbase
vibrational coupling. In the absence of such complicating perturbations
we would expect the C=O frequencies of both bases to be higher in the B[*]
structure than in the solvated mononucleotides or polynucleotides because
of weaker hydrogen bonding of carbonyl acceptors in the double helix than
in the solvated state (19). The fact that this is not the case supports
the notion that interbase vibrational coupling (18) also occurs in the B[*]
structure of poly(dG–dC). We note, however, that the two double-bond

frequencies observed here are not identical to those observed in the infrared (18) and Raman spectra (22) of the ribopolymer A* structure, poly(rG)·poly(rC), suggesting different interbase coupling in the two kinds of helix.

The strong Raman line at 1355 cm^{-1} in the B* structure has no counterpart in the B structure and thus shows up as a strong negative peak in the difference spectrum of Fig. 1. This frequency is due to a ring vibration of deuterated guanine (16) which exhibits high Raman intensity in B* structures (17). We have noted previously that the 1355 cm^{-1} peak is concealed in the spectrum of deuterated native DNA by a companion adenine ring mode near 1340 cm^{-1}, but is nicely uncovered in the DNA difference (B - B*) spectrum (8).

Fig. 2 shows the effects of deuteration of the high-salt structure of poly(dG-dC)·poly(dG-dC). We note that our Z spectrum is similar to those published previously (2,5), while the difference spectrum (Z - Z*) evidences large deuteration shifts of most Raman lines. The difference spectrum of Fig. 2 is qualitatively similar to the difference spectrum of Fig. 1, except that the peak maxima and minima are generally shifted to lower frequency in the former case. Those frequencies which are displaced are sensitive to the B-to-Z structure transition. Conspicuous among these are the aforementioned cytosine ring breathing mode and guanine ring mode, shifted respectively to 775 and 1480 cm^{-1} in the Z structures. On the other hand, Raman lines due to vibrations of the Z-DNA backbone, near 785-810 and 1090 cm^{-1}, show no significant deuteration shifts. The absence of deuteration shifts also characterizes the backbone vibrations of native B and A-DNA structures (8).

The difference spectra of Figs. 1 and 2 are clearly not identical in the double-bond region, a difference band occurring in the former at 1715 cm^{-1} and in the latter at 1695 cm^{-1}. Thus the C=O stretching modes of G and C in the two kinds of helix differ as a consequence of the different arrangements of hydrogen bonded bases in the two structures, including probable differences in propellor twist (3,4). In Table 1 we list the double-bond stretching frequencies of G and C that have been observed in Raman spectra of a number of deuterated helical structures. The C=O modes, here uncoupled from hydrogen bending modes (15), are sufficiently different in all cases to permit the structures to be distinguished from one another on this basis alone. (The broadly sloping feature in the difference spectrum of Fig. 2 between 300 and 600 cm^{-1} is due to

TABLE 1

CARBONYL GROUP STRETCHING FREQUENCIES
FROM RAMAN SPECTRA OF DEUTERATED GC STRUCTURES

Structure	Type	Frequencies[b](cm^{-1}) 2C=O,(C)	6C=O,(G)	Refs.
CMP+GMP[a]	-	(1650)	1670	15,21
poly(rC), helix	single strand	1650	-	7,12
5'rGMP, gel	tetramer	-	1665,(1697)	17
poly(rG), helix	tetraplex	-	1664,(1692)	17
poly(rG)·poly(rC)	A[*] duplex	(1650)	1699	22
poly(dG–dC)·poly(dG–dC)	B[*] duplex	(1635)	1688	This work
poly(dG–dC)·poly(dG–dC)	Z[*] duplex	(1634)	1662	This work

[a]The same frequencies are observed for ribo– and deoxyribo–nucleotides, nucleosides and their equimolar mixtures (22).
[b]Where two frequencies are listed, the less intense Raman line is given in parentheses.

incomplete solvent compensation and does not represent Z–DNA Raman scattering.)

Effects of the B–to–Z Structure Transition.

Fig. 3 shows the effects of the B–to–Z structure transition upon the Raman spectrum of poly(dG–dC)·poly(dG–dC). The shift of the guanine ring mode from 682 cm^{-1} to 625 cm^{-1} is certainly the most dramatic and perhaps the most useful for analytical purposes (5), but prominent guanine and cytosine lines throughout the 1200 to 1500 cm^{-1} region are also shifted, as are lines due to the backbone near 785–810 and 1090 cm^{-1}. Many of these spectral changes have been discussed previously (2,5,8). In particular, the Raman line at 1418 cm^{-1} in the B structure, assigned previously to methylene deformations of the deoxyribose residue and sensitive to the B–to–A structure transition (8), is also sensitive to the B–to–Z structure transition. Additionally, in the double–bond region of H_2O solutions we observe a clearcut shift of the 1715 cm^{-1} line of the B structure to 1695 cm^{-1} in the Z structure.

In D_2O solution the B[*]–to–Z[*] transition is again characterized most distinctively by a large shift to lower frequency of the guanine 682 cm^{-1} line. However, the Z[*] guanine mode is centered at 615 cm^{-1}, compared with

625 cm^{-1} in Z-DNA, which shows that this guanine ring mode is deuteration sensitive in Z structures but not in B structures. Clearly, the normal mode is qualitatively different in the two types of helix. (See further discussion, below.) Otherwise, most of the features of the difference spectrum of Fig. 4 have a close counterpart in the difference spectrum of Fig. 3, with the exception that the frequencies of maxima and minima are slightly lower in the deuterated forms. This is as expected for guanine and cytosine ring vibrations (15).

The carbonyl group frequencies in B* and Z* structures differ significantly by virtue of a shift of the guanine 6C=O stretching mode from 1688 cm^{-1} in the B* structure to 1662 cm^{-1} in the Z* structure (Table 1).

Conversely, Raman lines which exhibit the same frequencies in the two difference spectra (Figs. 3 and 4) can be confidently assigned to the deoxyribose phosphate backbone. Accordingly, the 829 and 1418 cm^{-1} peaks of B (and B*) structures, and the 790 and 1426 cm^{-1} peaks in Z (and Z*) structures are assigned to the DNA backbones. The same rationale permits assignment of the line at 748 cm^{-1} and the very weak shoulder at 810 cm^{-1} of both Z and Z* structures to the backbone of left-handed DNA. Further discussion of these assignments has been given by Prescott et al. (8).

Structural differences between B* and Z* structures can also be seen in the region of deoxyribosyl CH stretching vibrations, 2800-3000 cm^{-1}, in Fig. 4. The three lines of the low-salt conformer, at 2892, 2956 and 2970 cm^{-1}, coalesce to two lines in the high-salt form at 2894 and 2955 cm^{-1}. The aromatic CH stretching modes are poorly resolved in the high-salt spectrum. However, for the B* structure the lines at 3098, 3113 and 3128 cm^{-1} can be assigned to cytosine 4C-H, cytosine 5C-H and guanine 8C-H stretching, respectively (16).

Qualitative Identification of DNA Secondary Structures from Raman Spectra.

In Fig. 5 we show the region 550-850 cm^{-1} from high resolution Raman spectra of Z, B and A structures of DNA in both non-deuterated and deuterated forms. These spectra reveal the clearcut differences between the respective DNA structures and permit the assignments listed in Table 2. The data of Table 2 are proposed as characteristic Raman frequencies for the qualitative identification of different DNA structures.

Quantitative Determination of DNA Secondary Structure from Raman Intensities.

For quantitative applications we propose that the ratio of Z to B

TABLE 2

RAMAN LINES CHARACTERISTIC OF THE DNA BACKBONE IN A, B AND Z STRUCTURES

	Frequency(cm^{-1})	Intensity	Assignment or Origin[a]
A-DNA	807±3	strong	OPO antisymmetric + symmetric stretch
	1099	medium	PO_2^- symmetric stretch
	1415±3	medium	CH_2 deformation
B-DNA	784±3	strong	OPO symmetric stretch
	830±4	medium	OPO antisymmetric stretch
	1090	medium	PO_2^- symmetric stretch
	1420±2	medium	CH_2 deformation
Z-DNA	748	medium	OPO symmetric stretch
	792	weak	OPO antisymmetric stretch
	810	weak,shoulder	OPO antisymmetric stretch
	1095	medium	PO_2^- symmetric stretch
	1425±2	medium	CH_2 deformation

[a]Only the major contributor to the normal mode is listed. However, all phosphodiester modes involve some mechanical coupling with motions of adjacent ester carbons. (See refs. 23 and 24.)

conformers of guanine in DNA may be reliably calculated from the ratio of Raman intensities at 625 and 682 cm^{-1} (I_{625}/I_{682}). The basis for this proposal is the apparently equal intrinsic intensities of the 625 and 682 cm^{-1} lines when the spectra are normalized to the conformation-insensitive line at 1575 cm^{-1} (8). This fact is also illustrated by the B - Z difference spectra of Figs. 3 and 5. A similar conclusion was reached by Thamann et al. (5) from consideration of the intensities normalized to an independent internal standard (980 cm^{-1} line of sulfate ion). It is evident from the difference spectrum of Fig. 3 that the Raman intensities may be measured either by peak height or by band area since there are no significantly intense Raman lines which overlap the guanine ring modes in question. Further, the same arguments apply also to the intensity quotient I_{615}/I_{682} for D_2O solutions (cf. Figs. 4 and 5).

In order to substantiate the use of these intensity quotients we have prepared mixtures containing various molar percentages of Z-DNA (i.e. high-salt poly(dG-dC)·poly(dG-dC)) in aqueous 5'dGMP, recorded their Raman spectra, and measured the ratio I_{625}/I_{682} using both peak height and band area methods. Our results confirm a quantitative relationship between the Raman intensity ratio and the Z-to-B conformer ratio.

We have shown elsewhere (11) that the Raman intensity ratio I_{682}/I_{668} is a quantitative measure of the proportion of C2'-endo to C3'-endo, anti conformers of deoxyguanosine, i.e. a measure of the proportion of G residues distributed between B and A conformations. Thus, the present and earlier results together indicate the ability to determine by Raman spectroscopy whether guanine residues exist in regions of Z, B or A secondary structure.

The sensitivity of the guanine ring mode to sugar pucker and anti/syn orientation about the glycosidic bond was first reported by Tsuboi and collaborators (20). Such conformation sensitivity is unusual among purine or pyrimidine ring frequencies. We believe it arises from the extraordinary low frequency of the G ring breathing mode, which permits coupling with bond stretching vibrations of the furanose ring through the Cl'-N9 linkage (11). (The corresponding ring mode of adenines and hypoxanthines occurs near 725 cm^{-1} (15).) The extent of base-sugar coupling and thus the nature of the normal mode evidently differ among the various deoxyguanosine conformers so far examined, as illustrated by the deuteration effect of the Z marker line (shift from 625 to 615 cm^{-1}), but the lack of a deuteration effect for the B marker line (682 cm^{-1}).

CONCLUSIONS

The Raman spectra of poly(dG-dC)·poly(dG-dC) in D_2O solutions of low (0.1M) and high (4.0M) salt correspond to the B-DNA and Z-DNA structures reported previously for the respective H_2O solutions (2,5). Raman difference spectra of both H_2O and D_2O solutions indicate that the relative intensities of the guanine ring breathing mode (I_{625}/I_{682} and I_{615}/I_{682} for H_2O and D_2O solutions, respectively), measured by either peak height or band area, may be exploited to determine quantitatively the ratio of Z to B structures present in a GC-containing DNA. We estimate the reliability of the method as ±5% when no interfering bands from impurities or other molecular constituents are present. In combination with previous results on model compounds exhibiting B and A conformations

(11), the Raman intensities of guanine ring modes may be used to distinguish whether the base residue exists in regions of A (C3'-endo, anti), B (C2'-endo, anti) or Z (C3'-endo, syn) secondary structure. Since the present correlations are derived from the sensitivity of the Raman frequency to sugar pucker (C2'-endo vs. C3'-endo) and glycosidic bond orientation (anti vs. syn), they may be applied to oligomers or monomers as well as to polynucleotides for identification of molecular conformations.

In addition to the guanine "reporter" frequencies, the spectra of B and Z-DNA, as well as A-DNA (8), exhibit several lines which are derived from the deoxyribose-phosphate backbone and which are measurably different for each secondary structure. Thus the ability to detect Z, B and A structures does not depend solely upon the presence of guanine residues in the nucleic acid chain. However, the characteristic Raman lines of the different DNA backbone structures are not sufficiently separated from one another to allow rigorous quantitative analysis using present methods. The data of Fig. 5 indicate, nevertheless, that the Raman lines of the backbone can provide semi-quantitative estimates of Z, B and A structure domains.

The Raman lines in the double-bond region of D_2O solution spectra, which are assigned to C=O stretching frequencies of G and C, are also useful analytically to identify different hydrogen-bonded base pairing schemes by analogy with known GC structures. Although the lines in this spectral region are generally weaker than those mentioned above, computer generated difference spectra should permit their use for both qualitative and quantitative assessment of GC interactions. In any case, the present results (Table 1) suggest to us that, among the known DNA duplex structures which are stable in aqueous solutions, GC hydrogen bonding interactions are strongest in Z helices, intermediate in B helices and weakest in A helices.

A potentially important application of the present D_2O solution results on high-salt poly(dG-dC)·poly(dG-dC) is for the identification of Z-DNA sequences in protein-DNA complexes. The Z*-DNA marker occurs at a position (615 cm^{-1}) where protein Raman lines do not occur. The same is not true for corresponding H_2O solutions where the interference of a phenylalanine ring mode (625 cm^{-1}) could prevent the detection of the Z conformer.

REFERENCES

1. Pohl, F. M. and Jovin, T. M. (1972) J. Mol. Biol. 67, 375-396.
2. Pohl, F. M., Ranade, A. and Stockburger, M. (1973) Biochim. Biophys. Acta 335, 85-92.
3. Wang, A. H.-J., Quigley, G. J., Kolpak, F. J., Crawford, J. L., van Boom, J. H., van der Marel, G. and Rich, A. (1979) Nature 282, 680-686.
4. Crawford, J. L., Kolpak, F. J., Wang, A. H.-J., Quigley, G. J., van Boom, J. H., van der Marel, G. and Rich, A. (1980) Proc. Natl. Acad. Sci. USA 77, 4016-4020.
5. Thamann, T. J., Lord, R. C., Wang, A. H.-J. and Rich, A. (1981) Nucl. Acids Res. 9, 5443-5457.
6. Wartell, R. M., Klysik, J., Hillen, W. and Wells, R. D. (1982) Proc. Natl. Acad. Sci. USA 79, 2549-2553.
7. Prescott, B., Gamache, R., Livramento, J. and Thomas, G. J., Jr. (1974) Biopolymers 13, 1821-1845.
8. Prescott, B., Steinmetz, W. and Thomas, G. J., Jr. (1983) Biopolymers, in press.
9. Erfurth, S. C., Kiser, E. J. and Peticolas, W. L. (1972) Proc. Natl. Acad. Sci. USA 69, 938-941.
10. Erfurth, S. C. and Peticolas, W. L. (1975) Biopolymers 14, 247-264.
11. Benevides, J. M., LeMeur, D. and Thomas, G. J., Jr. (1983) Biopolymers, submitted.
12. Chou, C. H. and Thomas, G. J., Jr. (1977) Biopolymers 16, 765-789.
13. Li, Y., Thomas, G. J., Jr., Fuller, M. and King, J. (1981) Prog. Clin. Biol. Res. 64, 271-283.
14. Savitzky, A. and Golay, M. J. (1964) Anal. Chem. 36, 1627-1638.
15. Lord, R. C. and Thomas, G. J., Jr. (1967) Spectrochim. Acta 23A, 2551-2591.
16. Lane, M. J. and Thomas, G. J., Jr. (1979) Biochemistry 18, 3839-3846.
17. Rice, J., Lafleur, L., Medeiros, G. C. and Thomas, G. J., Jr. (1973) J. Raman Spectrosc. 1, 207-215.
18. Howard, F. B., Frazier, J. and Miles, H. T. (1969) Proc. Natl. Acad. Sci. USA 64, 451-458.
19. Bellamy, L. J. (1975) The Infrared Spectra of Complex Molecules, Vol. 1, Third Edition, Wiley, N.Y.
20. Nishimura, Y., Tsuboi, M., Kato S. and Morokuma, K. (1982), in Raman Spectroscopy, Linear and Non-Linear, J. Lascombe and P. V. Huong, Eds., Wiley, N.Y., pp. 703-704.
21. Lord, R. C. and Thomas, G. J., Jr. (1967) Biochim. Biophys. Acta 142, 1-11.
22. Lafleur, L., Rice, J. and Thomas, G. J., Jr. (1972) Biopolymers 11, 2423-2437.
23. Brown, E. B. and Peticolas, W. L. (1975) Biopolymers 14, 1259-1271.
24. Martin, J. C. and Wartell, R. M. (1982) Biopolymers 21, 499-512.